
Sparse is Enough in Fine-tuning Pre-trained Large Language Models

Weixi Song^{*1} Zuchao Li^{*1,2} Lefei Zhang^{1,2} Hai Zhao³ Bo Du^{1,2}

Abstract

With the prevalence of pre-training-fine-tuning paradigm, how to efficiently adapt the pre-trained model to the downstream tasks has been an intriguing issue. **Parameter-Efficient Fine-Tuning (PEFT)** methods have been proposed for low-cost adaptation. Although PEFT has demonstrated effectiveness and been widely applied, the underlying principles are still unclear. In this paper, we adopt the PAC-Bayesian generalization error bound, viewing pre-training as a shift of prior distribution which leads to a tighter bound for generalization error. We validate this shift from the perspectives of oscillations in the loss landscape and the quasi-sparsity in gradient distribution. Based on this, we propose a gradient-based sparse fine-tuning algorithm, named **Sparse Increment Fine-Tuning (SIFT)**, and validate its effectiveness on a range of tasks including the GLUE Benchmark and Instruction-tuning. The code is accessible at <https://github.com/song-wx/SIFT>.

1. Introduction

With the prevalent pre-training-fine-tuning paradigm, Large Language Models (LLMs) pre-trained on a large corpus can be effectively adapted to the specific downstream domain. However, fine-tuning all parameters for LLMs is prohibitively expensive. Toward efficient adaptation from pre-trained LLMs to downstream tasks, several parameter-

efficient fine-tuning methods have been proposed (Houlsby et al., 2019; Zaken et al., 2022; Li & Liang, 2021; Hu et al., 2021; Zhang et al., 2023; Dettmers et al., 2023), which can achieve the performance close to or even surpass that of full fine-tuning with lower costs.

Although these methods have demonstrated their effectiveness to some extent and have been widely applied, the underlying principles are still unclear. Li et al. (2018a) points out that over-parameterized networks have a lower intrinsic dimension, i.e. they can achieve 90% or even 100% of the full parameter performance by training only fewer parameters than the full parameter, which is the motivation of LoRA (Hu et al., 2021). A natural question is:

What causes pre-trained language models to have the lower intrinsic dimension?

To answer this question, we first need to understand what changes occur from random initialization to pre-trained initialization. As indicated in Devlin et al. (2019), pre-trained models rapidly generalize to downstream data through fine-tuning. Thus, compared to random initialization, the generalization error of pre-training initialization seems to be controlled by a tighter bound. Therefore, we shed a spotlight on a classic PAC-Bayesian generalization error bound, first proposed by McAllester (2003) and refined by Maurer (2004); Catoni (2007); Thiemann et al. (2017). In contrast to general PAC bounds that only consider the complexity of the hypothesis space, typically measured by VC-dimension (Vapnik, 1991) or Rademacher complexity (Bartlett & Mendelson, 2002), PAC-Bayesian bounds jointly consider a less accurate prior probability distribution for parameters and a more precise data-based posterior distribution. We view pre-training as a shift of prior, where pre-training, by learning language features such as grammar and syntax on a large corpus, moves the model away from sub-manifolds of non-expressive parameters in the parameter space. Pre-training initialization is equivalent to assigning relatively low probabilities in the prior for non-expressive parameters. In contrast to random initialization, which assigns equal probabilities in the prior to all parameters, the KL divergence between the pre-trained prior and the data-based posterior is lower, as shown in Figure 1. Therefore, pre-trained models have a tighter generalization error bound. We validate this prior shift through investigating changes in the loss landscape and gradient distribution after pre-training. From random initialization to pre-trained initialization, the

^{*}Equal contribution This work was supported by the National Natural Science Foundation of China (No.62306216), the Natural Science Foundation of Hubei Province of China (No.2023AFB816), the Fundamental Research Funds for the Central Universities (No.2042023kf0133), National Natural Science Foundation of China [No.72074171] [No.72374161]. ¹National Engineering Research Center for Multimedia Software, School of Computer Science, Wuhan University, Wuhan, 430072, P. R. China ²Hubei LuoJia Laboratory, Wuhan 430072, P. R. China ³Department of Computer Science and Engineering, Shanghai Jiao Tong University, Shanghai, 200240, P. R. China. Correspondence to: Zuchao Li <zeli-charlie@whu.edu.cn>.

loss landscape transitions from flat oscillations to sharp oscillations, and the gradient exhibits a quasi-sparse property, where partial components dominate the majority of the gradient norm.

Based on this, we propose a gradient-based sparse update scheme called **Sparse Increment Fine-Tuning (SIFT)**. Unlike existing PEFT methods, such as LoRA (Hu et al., 2021), Adapter (Houlsby et al., 2019), Prefix-Tuning (Li & Liang, 2021), that require plugging in additional modules, SIFT does not alter the model’s structure. Instead, it inserts hook functions into back propagation to acquire sparse gradients and perform in-place sparse updates on the parameters, as illustrated in Figure 5. We validate its effectiveness on a range of tasks, including the GLUE Benchmark and Instruction-tuning.

In summary, the contributions of this paper are as follows:

- To our best knowledge, this is the first time analyzing the generalization of pre-trained models from the perspective of PAC-Bayesian Bounds. We validate the prior shift of pre-trained models by investigating the changes of loss landscapes and gradient distributions.
- We propose a gradient-based sparse fine-tuning algorithm, an efficient and simple PEFT method, which need no additional plug-in modules and achieve efficient fine-tuning by updating only partial components.
- We introduce a memory-efficient implementation for SIFT by utilizing hooks during backward propagation, which could potentially be implemented at the lower level of deep learning training frameworks like PyTorch (Paszke et al., 2017). This paves the way for more streamlined and efficient fine-tuning.

2. Related Work

Parameter-efficient Fine-tuning: To apply pre-trained models more efficiently to downstream tasks, Houlsby et al. (2019) proposes parameter-efficient transfer learning by inserting a bottleneck structure between different layers of the pre-trained model. During fine-tuning, the pre-trained parameters remain unchanged, and only the bottleneck layers are updated. Zaken et al. (2022) shows that training only bias terms and task-specific modules during fine-tuning can also adapt pre-trained models effectively to downstream tasks. Prefix-tuning (Li & Liang, 2021) adapts pre-trained models to downstream tasks by prepending trainable continuous tokens (Prefixes) to the input and hidden states of each Transformer layer. LoRA (Hu et al., 2021) freezes the weights of pre-trained models and injects trainable rank decomposition matrices into each layer of the Transformer architecture. Following the proposal of LoRA, several LoRA-based improvements have been introduced, including AdaLoRA (Zhang et al., 2023), which adaptively allocates

parameter budgets based on the importance of weight matrices, and QLoRA (Dettmers et al., 2023), which further reduces the resource overhead through quantization techniques. The above PEFT methods, except for Bias-only which is a module sparse approach, are all adapted to the downstream tasks by introducing additional modules.

PAC-Bayesian Generalization Error Bounds: introduced by McAllester (1999; 2003), combines the advantage of Bayesian methods and PAC Learning, which allows for considering domain knowledge as a Bayesian prior without assuming the truth of the prior (McAllester, 2003). Early generalization error bounds only consider the complexity of the hypothesis space, measured by VC-dimension (Vapnik, 1991) and Rademacher complexity (Bartlett & Mendelson, 2002), which is nearly vacuous and trivial in the real neural network setting (Zhang et al., 2021). In contrast, PAC-Bayes methods reward models whose prior assigns higher probability to those hypotheses that are in line with train data, with a tighter control over generalization error.

3. Understanding Pre-training-fine-tuning from a Distribution-shift Perspective

The pre-training-fine-tuning paradigm has shown great success in numerous NLP tasks (Devlin et al., 2019). To our best knowledge, there is still no conclusive answer as to why pre-training can improve performances and generalization abilities in different tasks. In this section, we will adopt the PAC-Bayesian generalization error bounds and, from the perspective of the prior distribution shift, analyze the pre-training-fine-tuning paradigm in both theoretical and empirical aspects.

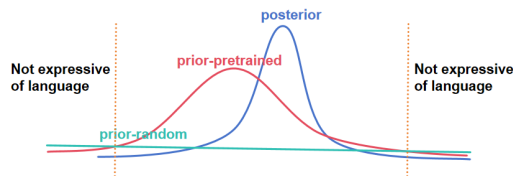


Figure 1. An intuitive explanation about prior distribution and posterior distribution. Random initialization is equivalent to assigning equal probabilities to hypotheses in the hypothesis space (the horizontal line referred as prior-random). Pretraining learns language features from extensive corpora, moving away from hypotheses that are not accurately expressive of language, equivalent to assigning them lower prior probabilities. Data-based, more precise posterior also have lower probabilities for hypotheses that fail to represent and understand language correctly. Therefore, compared to prior-random, the KL divergence between prior-pretrained and posterior is smaller.

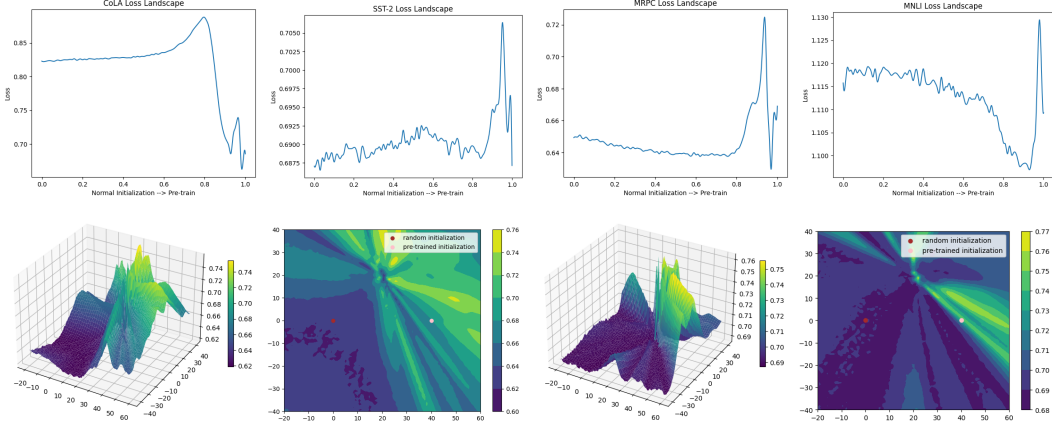


Figure 2. 1-D (up) and 2-D (down) visualization of the shift of the loss landscape from random initialization to pre-trained initialization. The figures show the loss landscape transitions from low amplitude oscillations to high amplitude oscillations.

3.1. PAC-Bayesian Generalization Error Bounds

For a fixed architecture of the deep learning model, models with different parameter values (i.e., hypotheses) collectively form the hypothesis space. Any hypothesis h in the hypothesis space \mathcal{H} can be represented as $h = \sum_{i=1}^N h_i e_i$, where N is the total number of parameters, e_i is akin to the definition of the standard basis (with the i^{th} component being 1 and the rest being 0), and h_i represents the value of the model h on the i^{th} component. Hence, a straightforward conclusion is that $|\mathcal{H}| \leq N$, and subsequent discussions are based on the premise that the hypothesis space is finite.

Let the empirical risk of h be $\hat{\mathcal{R}}(h) = \frac{1}{n} \sum_{i=1}^n l(h, s_i)$, and the population risk be $\mathcal{R}(h) = \mathbb{E}_{s \sim \mathcal{S}} [l(h, s)]$, where s_i is independently sampled from the identical data distribution \mathcal{S} , n represents the number of samples, l is a bounded loss function, and for simplicity, $l(h, s) \in [0, 1]$. The generalization error is defined as $\Delta(h) = \hat{\mathcal{R}}(h) - \mathcal{R}(h)$.

In this setting, with a probability at least $1 - \delta$, the population risk $\hat{\mathcal{R}}(h)$ satisfies:

$$\forall h \in \mathcal{H}, \hat{\mathcal{R}}(h) \leq \mathcal{R}(h) + \sqrt{\frac{\log(|\mathcal{H}|) + \log(1/\delta)}{2n}} \quad (1)$$

If we consider a probability distribution \mathcal{P} regarding hypotheses, referred to as a prior (McAllester, 1998), then with a probability of at least $1 - \delta$,

$$\forall h \in \mathcal{H}, \hat{\mathcal{R}}(h) \leq \mathcal{R}(h) + \sqrt{\frac{\log(1/\mathcal{P}(h)) + \log(1/\delta)}{2n}} \quad (2)$$

A most trivial prior is to assume that all hypotheses are equally likely, i.e., $\forall h \in \mathcal{H}, \mathcal{P}(h) = 1/\log(|\mathcal{H}|)$. In this case, the inequality 2 degenerates to 1. But the parameters are certainly not uniformly distributed. For natural language processing tasks, without considering specific data, parameters that can accurately represent fundamental language features such as grammar and semantics should be assigned

a higher probability. We refer to this as a weakly informative prior, which conveys partial information.

If we consider a more precise distribution \mathcal{Q} , which characterizes the probability distribution of the parameters based on specific data, referred to as a posterior, then we have the following bound on the population risk, first introduced by McAllester (2003), with a probability at least $1 - \delta$:

$$\mathbb{E}_{h \sim \mathcal{Q}} [R(h)] \leq \mathbb{E}_{h \sim \mathcal{Q}} [\hat{R}(h)] + \sqrt{\frac{\mathbb{KL}(\mathcal{Q}||\mathcal{P}) + \log(n/\delta) + 2}{2n - 1}} \quad (3)$$

The formula 3 indicates that the smaller KL divergence between the prior and the posterior, the tighter control there is on the generalization error. A more detailed introduction of the above theorems can be found in Appendix A.

Pre-training language models aims to learn grammar, semantics, and other basic language features (referred to as a prior) from a large corpus through masking or auto-regressive methods, steering the model away from parameters that cannot correctly understanding and convey language. Therefore, pre-trained initialization of the model is equivalent to assigning lower probabilities to such parameters in the prior. Those parameters are naturally incapable of handling various tasks related to language correctly, so they should also have lower probabilities in the data-based posterior. As shown in Figure 1, pre-trained initialization considering basic language features is closer to the distribution of the data-based on posterior compared to random initialization. This closeness results in lower KL divergence and, consequently, a tighter upper bound on generalization error, allowing the population risk to consistently decrease along with the reduction of empirical risk during training.

In Sections 3.2 and 3.3, we validate these differences between random and pre-trained initialization from both the loss landscape and gradient distribution perspectives.

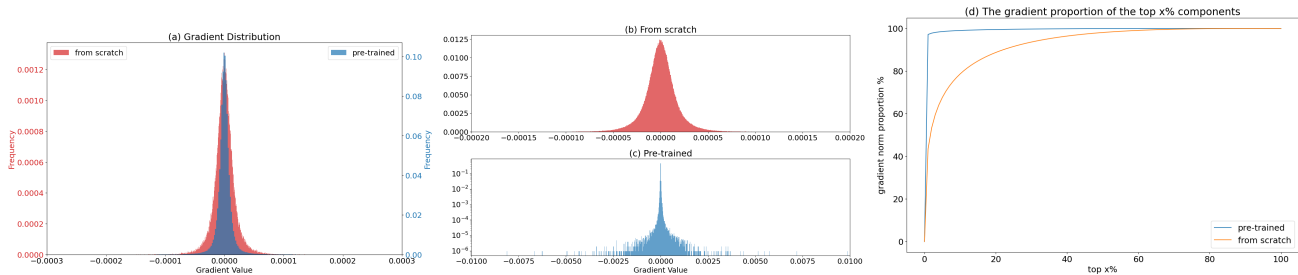


Figure 3. (a) depicts the gradient distribution of parameters in one layer of RoBERTa-Large on the MNLI dataset, showing different gradient distributions of the models trained from scratch and from pre-trained. Both distribution are approximately presenting a bell-shaped distribution similar to a normal distribution with a mean of zero. (b) and (c) are drawn on their respective scales, showing that compared to the model trained from scratch, the gradients of the pre-trained model are more concentrated around zero while they exist much larger gradient values. (d) illustrates the gradient proportion of the top x% components, indicating that the gradients of the pre-trained model hold a more extreme property, dominating 99% of the complete gradient norm with only 1% of the parameters.

3.2. Visualization of Loss Landscape

Loss landscape is a high-dimensional geometry which is completely determined as soon as a dataset and the network structure are specified (Li et al., 2018a), reflecting the relationship between the loss and parameters. For high-dimensional geometries such as loss landscapes, it is not possible to imagine and understand their geometric properties as intuitively as in low-dimensional shapes. Despite the difficulty in understanding such high-dimensional geometries, researchers have proposed methods to project high-dimensional loss surfaces into low-dimensional space, including one-dimensional visualization (Goodfellow et al., 2015; Smith & Topin, 2017) and two-dimensional visualization (Li et al., 2018b), in order to easily understand and study some of the properties of loss landscapes.

In exploring the shift of the loss landscape from random initialization to pre-trained initialization, we note θ_0 as the randomly initialized parameters and θ_1 as the pre-trained parameters. Goodfellow et al. (2015) plots the loss landscape curve from θ_0 to θ_1 by linearly sampling and interpolating the network parameters between θ_0 and θ_1 , the loss curve f is defined as:

$$f(\alpha) = \mathcal{L}(\theta_0 + \alpha\delta)$$

where $\alpha \in [0, 1]$ and δ is $\theta_1 - \theta_0$ that represents a direction. The two-dimensional loss surface f is plotted similarly to the one-dimensional one, determined by a starting point and two directions:

$$f(\alpha, \beta) = \mathcal{L}(\theta_0 + \alpha\delta_1 + \beta\delta_2).$$

In our setting, $\delta_1 = \theta_1 - \theta_0, \alpha \in [-0.5, 1.5], \beta \in [-1, 1]$, when $\alpha = 0, \beta = 0$, the model is in the random initialization state, and when $\alpha = 1, \beta = 0$, the model is in the pre-trained state. We use a method similar to Li et al. (2018b)

to construct the direction δ_2 to avoid the scaling effect between different components, multiplying δ_1 by a Gaussian random number points by points, i.e. $\delta_{2_i} = d_i * \delta_{1_i}$, where d_i follows a normal distribution. We investigate the shift of the loss landscape using RoBERTa-base (Liu et al., 2019) on a range of tasks at GLUE, which are shown in Figure 2. A prior idea would be that pre-trained models are more efficient at adapting to downstream tasks than training from scratch because the knowledge learned during pre-training reduces the initial loss. However, a striking fact is that pre-training does not make all tasks have lower losses than random initialization at the beginning of fine-tuning, e.g. MNLI, MRPC, etc. Instead, for most tasks, there are extremely higher losses than random initialization around the pre-trained initialization. A common feature of the loss landscape is that the oscillations of the loss around random initialization are generally small in magnitude, whereas the loss oscillations around pre-training are sharp, i.e. after a valid pre-training process, the loss landscape shifts from low amplitude oscillations to high amplitude oscillations. Since the 1-D and 2-D loss landscapes are projections of the original loss landscape, the special states exhibited in the low-dimensional projections reflect the general property of the high-dimensional space. A flat loss landscape implies a balanced influence among dimensions (corresponding to a uniform distribution prior). During parameter changes, the mutual constraints among dimensions lead to a smooth variation in loss. On the other hand, intense oscillations in loss landscape indicate that certain dimensions dominate the changes of the loss, suggesting an inconsistency in the probability distribution among dimensions (corresponding to the bell-shaped distribution in Figure 1).

3.3. Quasi-Sparse Gradient Distribution

Ye et al. (2020); Wiedemann et al. (2020) take the assump-

tion that the distribution of the parameter gradients approximates a normal distribution. In Figure 3, we plot the gradient distribution of one parameter in RoBERTa-Large on the MNLI dataset and other parameters also have the similar property shown in the following description. Both the gradients of the model trained from scratch and from pre-trained show a bell-shaped distribution with a mean of near zero. Under the same histogram settings, the gradient distributions of from scratch and pre-trained models show a huge difference in frequency and value range. Figure 3(c) displays the pre-trained gradient distribution on a log-scale, where the majority of gradients are concentrated around zero, with only a very small portion having larger gradient values, and the maximum value of pre-trained is about two orders of magnitude higher than that from scratch. Figure 3(d) shows the gradient proportion of the components with the top $x\%$ absolute gradient value. The pre-trained gradient shows a more extreme property, where 1% of the components account for 99% of the total gradient norm. This severe imbalance in distribution exhibits a property similar to sparsity, which we refer to as Quasi-Sparse. The majority of information in the gradient space can be represented by a very small number of components.

Through pre-training, the model reaches a sub-manifold in the parameter space where the parameters are with higher distribution probabilities and can be expressive of language (corresponding to the bell-shaped distribution in Figure 1). Therefore, during the fine-tuning process on downstream tasks, it is only necessary to search within this manifold to find a good solution. This results in redundancy on most dimensions, manifested by smaller gradient values, which is also referred as a low intrinsic dimension of the objective loss landscape (Li et al., 2018a). This imbalance in distribution also explains the shift from low to high amplitude oscillation discussed in Section 3.2. With the same step size, a balanced distribution of gradients in each dimension would lead a more smooth change in loss, whereas in the case of an imbalanced distribution of gradients, the dimensions with extreme gradients will dominate the change in loss, resulting in strong oscillations.

Therefore, a natural question is whether updating only in these dimensions can effectively adapt the pre-trained model to downstream domains.

4. Methodology

We describe the design of Sparse Increment Fine-Tuning (SIFT), whose principle is to update only a part of the components of the parameters. Based on the similar subspace method in nonlinear optimization (Liu et al., 2021), we provide a mathematical definition related to SIFT. Finally, we propose a memory-efficient implementation for SIFT.

4.1. SIFT: Sparse Increment Fine-Tuning

We define the fine-tuned parameters as the sum of pre-trained parameters and an increment, $x_{ft} = x_{pt} + \Delta x$. Updating only a portion of the components means that Δx is a sparse matrix, hence we name this update method Sparse Increment Fine-Tuning (SIFT). Below, we will explain that due to the quasi-sparse gradient property of the pre-trained model, Δx can ensure sufficient descent of the loss.

The idea of only updating partial components of the parameters is similar to the subspace method for non-linear optimization (Liu et al., 2021). In SIFT, we aim to update only components with the top $x\%$ absolute values of the gradient, so the update direction will be in a subspace spanned by these components' dimensions. We adopt the definition in (Liu et al., 2021), where g_k^i is denoted as the i^{th} component of gradient g_k . Sorted in descending order of absolute value, the top $x\%$ components are selected:

$$\begin{aligned} |g_k^{i_1}| &\geq |g_k^{i_2}| \geq |g_k^{i_3}| \geq \dots \geq |g_k^{i_m}|, \\ m &= \lfloor x\% * n \rfloor, \\ n &\text{ is the number of } g_k \text{ components} \end{aligned}$$

Therefore, the update direction d are in the subspace $\mathcal{S} = \text{span}\{e^{i_1}, e^{i_2}, \dots, e^{i_n}\}$, called the τ -steepest coordinates subspace, where e_i refers to the i^{th} standard basis. Based on this, we define the steepest descent direction as sufficiently descending, when,

$$\min_{d \in \mathcal{S}} \frac{d^T g_k}{\|d\|_2 \|g_k\|_2} \leq -\frac{\tau}{n}$$

That is, the descent direction d is sufficiently close to the negative gradient direction. If $(g_k^{\tau+1})^2 \leq \epsilon \sum_{j=1}^{\tau} (g_k^j)^2$, we can further obtain the following estimate,

$$\min_{d \in \mathcal{S}} \frac{d^T g_k}{\|d\|_2 \|g_k\|_2} \leq -\frac{1}{\sqrt{1 + \epsilon(n - \tau)}}$$

As discussed in section 3.2, for the gradients of pre-trained models, a few components dominate most of the gradient norm, allowing us to obtain a sufficiently small ϵ with a relatively small τ , ensuring that the direction d chosen from the subspace \mathcal{S} is sufficiently descending.

Due to the limitation of computational cost, we usually cannot obtain the gradients over the complete data. Instead, stochastic gradient type methods typically take a mini-batch sampled from the full data. Without the complete gradient information, SIFT uses the gradient from the first batch (or first several batches by using gradient accumulation) as an estimate of the complete gradient and selects the components to be updated based on this. A natural question arises: do the components selected based on the gradient of the first batch still effectively represent the full gradient information in subsequent batches? That is, whether there will

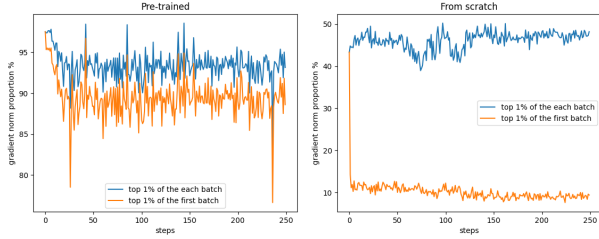


Figure 4. (Left) compares the difference in the proportion of gradients accounted for by two different top 1% component selection methods: the top 1% of the current batch and the top 1% of the first batch. Although sticking with the first batch’s top 1% as opposed to selecting the top 1% of the current batch results in some reductions of gradient information, the difference remains within an acceptable range. Avoiding frequent changes of components can improve training efficiency and preserve the historical information of Adam-like optimizers. In contrast, (Right) shows the gradient proportion variation in the model trained from scratch, where fixing the top 1% of the first batch leads to a greater reduction of the gradient information.

be significant differences between the gradients of different batches. As shown in Figure 4, we compare the proportion of the top 1% components of each batch’s gradients with the proportion of the top 1% components of the first batch’s gradients. For pre-trained models, using the top x% components of the first batch does indeed result in some reduction of gradient information, but except for some outlier samples, the difference always remains within an acceptable level compared to the top 1% of the current batch. In contrast, the top 1% components of the first batch in models trained from scratch tend to lose more gradient information. Therefore, for efficiency, SIFT always updates the top x% components of the first batch in the whole training process. This approach enables the use of Adam-like optimizers that require historical state information, as frequent changes of components would result in the loss of their historical information. Appropriate periodic changes of the components that need to be updated is also an acceptable choice, and this could be one of the focus for future work.

4.2. A Memory-efficient Implementation of SIFT

The key to SIFT lies in obtaining gradients of partial components. Under existing deep learning frameworks (such as PyTorch (Paszke et al., 2017)), gradients of all parameters are able to be accessed only after backward propagation. A simple implementation of SIFT is to retrieve the gradients of partial components through indexing after all gradients have been calculated. However, as all gradients have already been stored, storing the gradients of partial components at this point does not reduce the memory overhead of gradient storage. The memory overhead during training mainly consists of four parts: parameters, gradients, optimizer states, and activation. Although this implementation does not reduce

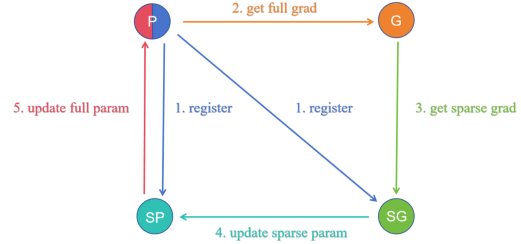


Figure 5. (1) For each parameter (P) that requires updating sparsely, we register a Sparse Parameter (SP) with the Sparse Gradient (SG), storing them in the form of values and indexes; (2) Acquire the computed gradient (G) by inserting a hook function; (3) Obtain partial components of the gradient through indexing to serve as the Sparse Gradient for the Sparse Parameter; (4) Use the Sparse Gradient to update the Sparse Parameter in the optimizer; (5) Use the Sparse Parameter to update the initial parameter.

storage overhead of gradients, it can significantly reduce that of the optimizer states.

Lv et al. (2023) proposes an alternative SGD method that reduces gradient storage by inserting a hook function, thereby fusing the gradient into the parameters as soon as the gradient is computed. Inspired by Lv et al. (2023), we propose a memory-efficient implementation of SIFT. As shown in Figure 5, we register a Sparse Parameter (SP) and corresponding Sparse Gradient (SG) for the parameters to be updated, only storing values and indexes for each. SP does not obtain SG through normal backward propagation. Instead, we inject a hook function into the parameters to capture the computed gradients and assign them to SG via indexing. SP with SG is updated through the normal optimizer, and finally, SP is integrated into the initial parameter P.

Table 1. Memory consumption of fine-tuning Llama 7B with different methods including full fine-tuning and SIFT in 5% sparsity rate. The data type of the model is bf16, the optimizers all use AdamW and are in fp32, and the sequence length and batch size are 2048 and 1. GC refers to whether gradient checkpointing is enabled or not.

	GC	PARAMS	GRAD	OPTIM STATES	ACTIVATION	TOTAL
FULL	✗	12.55	12.55	50.21	35.72	111.03
	✓				0.81	76.12
SIFT	✗	12.55	0.626	2.51	35.72	51.41
	✓				0.81	16.50

For x% sparse updates, we can simultaneously reduce the gradients and optimizer states to the original x%. Combined with techniques such as mixed-precision training and gradient checkpointing, it is possible to fine-tune a 7B model on a single RTX 3090 24GB, as shown in Table 1.

Table 2. Performances of fine-tuned pre-trained RoBERTa-large with different methods on the GLUE benchmark. Num denotes the number of trainable parameters in the fine-tuning process, excluding the classifier. Similar to (Hu et al., 2021), we report the matched and mismatched accuracy for MNLI, Matthew’s correlation for CoLA, Pearson correlation for STS-B, and accuracy for other tasks. * indicates results reported in (Hu et al., 2021). The best results are highlighted in **bold** and the second best results are underlined.

MODEL	METHOD	NUM	MNLI	SST-2	MRPC	CoLA	QNLI	QQP	RTE	STS-B	AVG.
ROBERTA-LARGE	FULL [*]	355.0M	90.2	<u>96.4</u>	90.9	68.0	<u>94.7</u>	92.2	86.6	92.4	88.9
	ADPT ^{P*}	3.0M	90.2	96.1	90.2	<u>68.3</u>	94.8	91.9	83.8	92.1	88.4
	ADPT ^{P*}	0.8M	<u>90.5</u>	96.6	89.7	67.8	94.8	91.7	80.1	91.9	87.9
	ADPT ^{H*}	6.0M	89.9	96.2	88.7	66.5	<u>94.7</u>	<u>92.1</u>	83.4	91.0	87.8
	ADPT ^{H*}	0.8M	90.3	96.3	87.7	66.3	<u>94.7</u>	91.5	72.9	91.5	86.4
	LoRA [*]	0.8M	90.6	96.2	90.2	68.2	94.8	91.6	85.2	<u>92.3</u>	<u>88.6</u>
	SIFT	0.8M	90.6	96.2	<u>90.4</u>	68.5	94.1	91.0	<u>85.9</u>	<u>92.3</u>	<u>88.6</u>

5. Experiments

Our evaluation mainly consists of two parts, targeting two cases: Natural Language Understanding (NLU) and Natural Language Generating (NLG). For NLU, we align with the evaluation of LoRA (Hu et al., 2021), selecting the GLUE Benchmark (Wang et al., 2019) as our evaluation dataset, and compare it with the data reported in (Hu et al., 2021). For NLG, to validate the effectiveness of SIFT on much larger models, we choose instruction-tuning as our test case. We adopt Llama (Touvron et al., 2023) as our backbone models, use the alpaca dataset (Taori et al., 2023) for instruction-tuning, and conduct evaluations on benchmarks such as MMLU (Hendrycks et al., 2021) and HumanEval (Chen et al., 2021). In the experiments, similar to (Hu et al., 2021), we only consider updating the parameters in the self-attention modules. By adjusting the sparsity rate of SIFT, we ensure a consistent number of trainable parameters. See Appendix B for detailed hyper-parameter settings, categories scores of MMLU and generated samples of HumanEval. In Section 5.3, we conduct further experimental analysis towards SIFT. Since SIFT selects components to update through gradient analysis, we compare SIFT with random component selection in Section 5.3.1. Additionally, as we heuristically choose to perform sparse updates on q,k,v and o, we compare the specific performance of applying SIFT in different parameters. Finally, in Section 5.3.2, we explore the impact of sparsity rate on the downstream task, investigating what is the limit of sparsity rate required for an acceptable performance in the downstream task. The evaluation includes the following baselines:

Full fine-tune: All pre-trained parameters are updated.

Adapter: (Houlsby et al., 2019) proposes to adapt pre-trained models to downstream tasks by inserting trainable Adapter modules into the self-attention layers while keeping the pre-trained parameters frozen. These modules have a bottleneck structure with non-linear function. We denote this original version as Adpt^H. Based on (Houlsby et al.,

Table 3. Performances of fine-tuned Llama on Alpaca dataset with different methods. We present the accuracy on the MMLU task under zero-shot setting, as well as the pass@1 and pass@10 metrics on the HumanEval task.

MODEL	METHOD	NUM	MMLU	HUMANEval
LLAMA-7B	VANILLA	\	32.7	11.3/16.5
	FULL	6.74B	42.0	11.1/19.5
	LoRA	0.32B	<u>40.7</u>	11.8/20.1
	SIFT	0.32B	<u>40.7</u>	<u>11.6/20.7</u>
LLAMA-13B	VANILLA	\	43.6	14.3/24.4
	FULL	13.0B	48.8	15.7/22.0
	LoRA	0.5B	<u>46.7</u>	14.6/25.6
	SIFT	0.5B	<u>46.7</u>	<u>15.5/26.2</u>
LLAMA-33B	VANILLA	\	54.3	20.9/36.0
	LoRA	0.98B	55.9	21.6/33.5
	SIFT	0.96B	<u>55.7</u>	24.1/37.2

2019), (Pfeiffer et al., 2021) proposed a more efficient version of the Adapter modules, referred to as Adpt^P.

LoRA(Hu et al., 2021): freezes the weights of the pre-trained model and adds trainable rank decomposition matrices in parallel to each layer of the Transformer architecture.

5.1. GLUE Benchmark

We evaluate SIFT on the GLUE benchmark (Wang et al., 2019). We select RoBERTa (Liu et al., 2019) as the backbone model for testing. The general experimental setup is consistent with (Hu et al., 2021) and we apply a 0.8% sparsity rate with SIFT to the Query, Key, Value, and Output projection in the self-attention module to ensure the number of trainable parameters is consistent with the compared baselines. Table 2 reports the results of pre-trained RoBERTa-Large with different fine-tuning methods on the GLUE benchmark and the number of trainable parameters (excluding the classifier). The results of each run are taken from the best epoch. Table 2 reveals that SIFT performs competitive on the GLUE benchmark compared to full fine-tuning and other PEFT methods.

Table 4. Performances of applying SIFT and random selection on different parameters. W_q, W_k, W_v, W_o represent the query, key, value, and output parameters in the attention module respectively and W_{All} denotes all parameters in the attention module (excluding LayerNorm).

TYPE	WEIGHT	NUM	RTE	MRPC	AVG.
SIFT	W_V	0.81M	<u>85.9</u>	90.4	88.0
	$W_{Q,V}$	0.81M	85.2	<u>90.2</u>	87.7
	$W_{Q,K,V}$	0.83M	84.8	88.7	86.8
	$W_{Q,K,V,O}$	0.80M	<u>85.9</u>	90.4	88.0
	W_{All}	0.80M	86.6	89.0	<u>87.8</u>
RANDOM	W_V	0.81M	<u>83.0</u>	<u>89.2</u>	<u>86.1</u>
	$W_{Q,V}$	0.81M	82.3	89.0	85.7
	$W_{Q,K,V}$	0.83M	81.9	87.5	84.7
	$W_{Q,K,V,O}$	0.80M	83.8	89.5	86.5
	W_{All}	0.80M	<u>83.0</u>	88.2	85.6

5.2. Instruction-tuning

Wei et al. (2022) proposes to perform supervised fine-tuning on top of pre-trained language models to make them align instructions and generate more meaningful content. Taori et al. (2023) fine-tunes pre-trained Llama on a 52k instruction-following dataset (Alpaca), which is generated by the technique introduced by Wang et al. (2023). We fine-tune Llama with Alpaca in different ways including full fine-tuning, LoRA and our SIFT. We evaluate language models on two benchmarks including MMLU and HumanEval. For MMLU, the evaluation metric is the accuracy of the generating answer in zero-shot setting, while HumanEval is evaluated by pass@1 and pass@10 metric. Higher values are better for all metrics. Table 3 demonstrates that sparse structures like SIFT can inject knowledge into pre-trained LLMs and exhibit a competitive performance.

5.3. Further Analysis

We primarily conduct further experimental analysis towards SIFT involving comparison of performance differences when applying SIFT on different parameters, as well as the differences between SIFT gradient-based component selection and random selection. Finally, we discuss the impact of the sparsity rate on the performance of downstream tasks.

5.3.1. SIFT VS. RANDOM

SIFT selects the component with the highest absolute gradient value in the first batch for the subsequent updates. A natural question arises: does this selection have an advantage over random selection? Additionally, in previous experiments, we heuristically choose the W_q, W_k, W_v and W_o in the attention modules for sparse updating. Under the condition of maintaining the same number of trainable parameters, including more modules to apply SIFT means

that each module has fewer trainable components. We want to know whether having fewer modules with more components or more modules with fewer components performs better in the fine-tuning process. In Table 4, we compare the performance of SIFT and random selection in updating different modules. We choose two small datasets from the GLUE benchmark, RTE and MRPC, for evaluation. The final performances do not show a consistent conclusion in the choice of different update modules. Therefore, balancing the number of components and modules, we choose to update W_q, W_k, W_v and W_o as our final choice. Compared to random selection, SIFT gradient-based selection method shows a clear advantage in the final performance of downstream tasks. However, although not as effective as SIFT in terms of performances, sparse updates in randomly selected components can still effectively adapt pre-trained models to downstream tasks, with only a small performance gap. This further confirms that due to the shift of the prior induced by pre-training, the model is away from non-expressive submanifolds in parameter space, resulting in redundancy across dimensions. Searching along partial dimensions is sufficient to find a relatively good solution.

5.3.2. SPARSITY RATE ANALYSIS

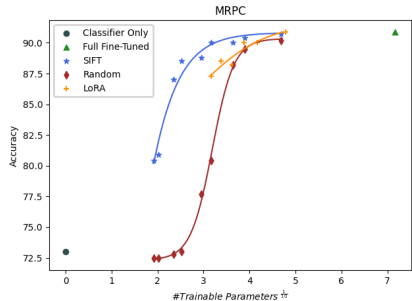


Figure 6. Performances of the fine-tuned pre-trained RoBERTa-Large vs different methods and the numbers of trainable parameters. Classifier only indicates that only the classifiers are fine-tuned, and the rest of the methods update the classifiers along with the parts of the pre-trained model.

We investigate the efficiency of different methods, that is, the trend of performance with the number of trainable parameters (budget). We compare performances of SIFT, Random selection and LoRA with varied budgets on MRPC dataset. Figure 5.3.2 show that SIFT is able to adapt the downstream task more efficiently in a less budget, while the performance gap between SIFT and LoRA is smoothed out as the budget increases. Consistent with the conclusion in Section 5.3.1, we find that when the number of parameters reaches a certain threshold, Random is also able to adapt the downstream task, but it is significantly inferior to SIFT and LoRA in terms of performances in less budgets.

6. Conclusion

In this paper, we adopt PAC-Bayesian bounds to analyze the pre-training-fine-tuning paradigm from the perspective of the prior distribution shift. We verify the shift of the prior through investigating differences of pre-trained models in loss landscapes and gradient distributions. Pre-trained models, compared to models trained from scratch, exhibit sharper oscillations in the loss landscape and gradients display a quasi-sparse property, where partial components dominates the majority of the gradient norm. Based on this, we propose a component-sparse fine-tuning strategy, named SIFT. We validate the effectiveness of using SIFT for fine-tuning on varied tasks including GLUE Benchmark and instruction-tuning for large language models. Furthermore, we have further discussions on SIFT, highlighting its efficiency from the comparison of different component selection methods and the performance trends of different methods as it varies with the number of trainable parameters.

References

- Bartlett, P. L. and Mendelson, S. Rademacher and gaussian complexities: Risk bounds and structural results. *Journal of Machine Learning Research*, 3(Nov):463–482, 2002.
- Catoni, O. Pac-bayesian supervised classification: the thermodynamics of statistical learning. *arXiv preprint arXiv:0712.0248*, 2007.
- Chen, M., Tworek, J., Jun, H., Yuan, Q., de Oliveira Pinto, H. P., Kaplan, J., Edwards, H., Burda, Y., Joseph, N., Brockman, G., Ray, A., Puri, R., Krueger, G., Petrov, M., Khlaaf, H., Sastry, G., Mishkin, P., Chan, B., Gray, S., Ryder, N., Pavlov, M., Power, A., Kaiser, L., Bavarian, M., Winter, C., Tillet, P., Such, F. P., Cummings, D., Plappert, M., Chantzis, F., Barnes, E., Herbert-Voss, A., Guss, W. H., Nichol, A., Paino, A., Tezak, N., Tang, J., Babuschkin, I., Balaji, S., Jain, S., Saunders, W., Hesse, C., Carr, A. N., Leike, J., Achiam, J., Misra, V., Morikawa, E., Radford, A., Knight, M., Brundage, M., Murati, M., Mayer, K., Welinder, P., McGrew, B., Amodei, D., McCandlish, S., Sutskever, I., and Zaremba, W. Evaluating large language models trained on code, 2021.
- Dettmers, T., Pagnoni, A., Holtzman, A., and Zettlemoyer, L. Qlora: Efficient finetuning of quantized llms, 2023.
- Devlin, J., Chang, M.-W., Lee, K., and Toutanova, K. Bert: Pre-training of deep bidirectional transformers for language understanding, 2019.
- Goodfellow, I. J., Vinyals, O., and Saxe, A. M. Qualitatively characterizing neural network optimization problems, 2015.
- Hendrycks, D., Burns, C., Basart, S., Zou, A., Mazeika, M., Song, D., and Steinhardt, J. Measuring massive multitask language understanding, 2021.
- Houlsby, N., Giurgiu, A., Jastrzebski, S., Morrone, B., de Laroussilhe, Q., Gesmundo, A., Attariyan, M., and Gelly, S. Parameter-efficient transfer learning for nlp, 2019.
- Hu, E. J., Shen, Y., Wallis, P., Allen-Zhu, Z., Li, Y., Wang, S., Wang, L., and Chen, W. Lora: Low-rank adaptation of large language models, 2021.
- Li, C., Farkhoor, H., Liu, R., and Yosinski, J. Measuring the intrinsic dimension of objective landscapes, 2018a.
- Li, H., Xu, Z., Taylor, G., Studer, C., and Goldstein, T. Visualizing the loss landscape of neural nets, 2018b.
- Li, X. L. and Liang, P. Prefix-tuning: Optimizing continuous prompts for generation, 2021.
- Liu, X., Wen, Z., Yuan, and Ya-Xiang. Sub-space methods for nonlinear optimization. *CSIAM Transactions on Applied Mathematics*, 2(4):585–651, 2021. ISSN 2708-0579. doi: <https://doi.org/10.4208/csiam-am.SO-2021-0016>. URL http://global-sci.org/intro/article_detail/csiam-am/19986.html.
- Liu, Y., Ott, M., Goyal, N., Du, J., Joshi, M., Chen, D., Levy, O., Lewis, M., Zettlemoyer, L., and Stoyanov, V. Roberta: A robustly optimized bert pretraining approach, 2019.
- Lv, K., Yang, Y., Liu, T., Gao, Q., Guo, Q., and Qiu, X. Full parameter fine-tuning for large language models with limited resources, 2023.
- Maurer, A. A note on the pac bayesian theorem. *arXiv preprint cs/0411099*, 2004.
- McAllester, D. A. Some pac-bayesian theorems. In *Proceedings of the eleventh annual conference on Computational learning theory*, pp. 230–234, 1998.
- McAllester, D. A. Pac-bayesian model averaging. In *Proceedings of the twelfth annual conference on Computational learning theory*, pp. 164–170, 1999.
- McAllester, D. A. Pac-bayesian stochastic model selection. *Machine Learning*, 51:5–21, 2003.
- Paszke, A., Gross, S., Chintala, S., Chanan, G., Yang, E., DeVito, Z., Lin, Z., Desmaison, A., Antiga, L., and Lerer, A. Automatic differentiation in pytorch. 2017.
- Pfeiffer, J., Kamath, A., Rücklé, A., Cho, K., and Gurevych, I. Adapterfusion: Non-destructive task composition for transfer learning, 2021.

- Smith, L. N. and Topin, N. Exploring loss function topology with cyclical learning rates. *ArXiv*, abs/1702.04283, 2017. URL <https://api.semanticscholar.org/CorpusID:18922459>.
- Taori, R., Gulrajani, I., Zhang, T., Dubois, Y., Li, X., Guestrin, C., Liang, P., and Hashimoto, T. B. Stanford alpaca: An instruction-following llama model. https://github.com/tatsu-lab/stanford_alpaca, 2023.
- Thiemann, N., Igel, C., Wintenberger, O., and Seldin, Y. A strongly quasiconvex pac-bayesian bound. In *International Conference on Algorithmic Learning Theory*, pp. 466–492. PMLR, 2017.
- Touvron, H., Lavril, T., Izacard, G., Martinet, X., Lachaux, M.-A., Lacroix, T., Rozière, B., Goyal, N., Hambro, E., Azhar, F., Rodriguez, A., Joulin, A., Grave, E., and Lample, G. Llama: Open and efficient foundation language models, 2023.
- Vapnik, V. Principles of risk minimization for learning theory. *Advances in neural information processing systems*, 4, 1991.
- Wang, A., Singh, A., Michael, J., Hill, F., Levy, O., and Bowman, S. R. Glue: A multi-task benchmark and analysis platform for natural language understanding, 2019.
- Wang, Y., Kordi, Y., Mishra, S., Liu, A., Smith, N. A., Khashabi, D., and Hajishirzi, H. Self-instruct: Aligning language models with self-generated instructions, 2023.
- Wei, J., Bosma, M., Zhao, V. Y., Guu, K., Yu, A. W., Lester, B., Du, N., Dai, A. M., and Le, Q. V. Finetuned language models are zero-shot learners, 2022.
- Wiedemann, S., Mehari, T., Kepp, K., and Samek, W. Dithered backprop: A sparse and quantized backpropagation algorithm for more efficient deep neural network training, 2020.
- Ye, X., Dai, P., Luo, J., Guo, X., Qi, Y., Yang, J., and Chen, Y. Accelerating cnn training by pruning activation gradients, 2020.
- Zaken, E. B., Ravfogel, S., and Goldberg, Y. Bitfit: Simple parameter-efficient fine-tuning for transformer-based masked language-models, 2022.
- Zhang, C., Bengio, S., Hardt, M., Recht, B., and Vinyals, O. Understanding deep learning (still) requires rethinking generalization. *Communications of the ACM*, 64(3):107–115, 2021.
- Zhang, Q., Chen, M., Bukharin, A., He, P., Cheng, Y., Chen, W., and Zhao, T. Adaptive budget allocation for parameter-efficient fine-tuning, 2023.

A. A Primer on PAC-Bayesian Generalization Error Bounds.

Due to limited pages of the main paper, all statements regarding PAC-Bayesian theory in the main text are kept as concise as possible. Therefore, in this section, we primarily address readers unfamiliar with PAC Learning or PAC-Bayesian Theorems. We will rigorously restate the theorems mentioned in the main paper, providing proofs for the simpler theorems and referencing related papers for the complex one.

The theorems in this section are introduced in previously published works. The presented overview here serves as a reminder and provides references for the readers as needed. The notation in this section remains consistent with that in the main paper.

Theorem A.1. *If \mathcal{H} is a finite hypothesis space, for any hypotheses $h \in \mathcal{H}$, any loss functions l bounded in $[0, 1]$, $0 < \delta < 1$, with a probability at least $1 - \delta$ over the selection of n i.i.d. samples,*

$$\hat{\mathcal{R}}(h) \leq \mathcal{R}(h) + \sqrt{\frac{\log(|\mathcal{H}|) + \log(1/\delta)}{2n}}$$

Proof. Using Hoeffding's inequality, for any $\epsilon > 0$,

$$\mathbb{P}\{\Delta(h) = \hat{\mathcal{R}}(h) - \mathcal{R}(h) \geq \epsilon\} \leq e^{-2n\epsilon^2}$$

Applying the Union Bound,

$$\mathbb{P}\{\exists h \in \mathcal{H}, \Delta(h) > \epsilon\} \leq \sum_{h \in \mathcal{H}} \mathbb{P}\{\Delta(h) > \epsilon\} \leq |\mathcal{H}|e^{-2n\epsilon^2}$$

Let $|\mathcal{H}|e^{-2n\epsilon^2} = \delta$, and solve the equation for ϵ , we have $\epsilon = \sqrt{\frac{\log(|\mathcal{H}|) + \log(1/\delta)}{2n}}$. □

Theorem A.2. (McAllester, 1998). *If \mathcal{H} is a finite hypothesis space, for any probability distribution \mathcal{P} over \mathcal{H} that assigns non-zero values, any hypotheses $h \in \mathcal{H}$, any loss functions l bounded in $[0, 1]$, $0 < \delta < 1$, with a probability at least $1 - \delta$ over the selection of n i.i.d. samples,*

$$\hat{\mathcal{R}}(h) \leq \mathcal{R}(h) + \sqrt{\frac{\log(1/\mathcal{P}(h)) + \log(1/\delta)}{2n}}$$

Proof. For any fixed $h \in \mathcal{H}$, considering the Chernoff Bound, we have

$$\mathbb{P}\{\Delta(h) > \sqrt{\frac{\log(1/\mathcal{P}(h)) + \log(1/\delta)}{2n}}\} = \mathbb{P}\{\Delta^2(h) > \frac{\log(1/\mathcal{P}(h)) + \log(1/\delta)}{2n}\} \leq \mathcal{P}(h)\delta$$

Then using the Union Bound,

$$\mathbb{P}\{\exists h \in \mathcal{H}, \Delta(h) > \sqrt{\frac{\log(1/\mathcal{P}(h)) + \log(1/\delta)}{2n}}\} \leq \sum_{h \in \mathcal{H}} \mathbb{P}\{\Delta(h) > \sqrt{\frac{\log(1/\mathcal{P}(h)) + \log(1/\delta)}{2n}}\} \leq \sum_{h \in \mathcal{H}} \mathcal{P}(h)\delta = \delta$$
□

Theorem A.3. (McAllester, 2003). *For any probability distribution \mathcal{P} on a possibly uncountable hypothesis space \mathcal{H} and any measurable loss function l , with a probability at least $1 - \delta$,*

$$\forall \mathcal{Q} \text{ on } \mathcal{H}, \mathbb{E}_{h \sim \mathcal{Q}}[R(h)] \leq \mathbb{E}_{h \sim \mathcal{Q}}[\hat{R}(h)] + \sqrt{\frac{\mathbb{KL}(\mathcal{Q}||\mathcal{P}) + \log(n/\delta) + 2}{2n - 1}}$$

A weak version of Theorem A.3 is first introduced in (McAllester, 1999). The complete proof of Theorem A.3 is in (McAllester, 2003). (Maurer, 2004; Catoni, 2007; Thiemann et al., 2017) have developed refinements on it.

B. Experimental Details

B.1. GLUE Benchmark Setting

The table 5 shows our hyper-parameters settings on the GLUE benchmark experiments.

Table 5. The hyperparameters of the GLUE Benchmark experiments

DATASET		MNLI	SST-2	MRPC	CoLA	QNLI	QQP	RTE	STS-B
METHOD									
	OPTIMIZER								
	WARMUP RATIO								
	LR SCHEDULE								
	BATCH SIZE								
	EPOCHS								
SIFT	LEARNING RATE	10	15	20	20	10	20	20	30
	WEIGHT DECAY	7E-5	7E-5	7E-5	7E-5	5E-5	7E-5	7E-5	8E-5
	MAX SEQ. LENGTH								
	SPARSITY RATE								
	SIFT MODULES								

B.2. Instruction-tuning Setting

The table 6 shows our hyper-parameters settings on the Instruction-tuning experiments.

Table 6. The hyper-parameters of the Instruction-tuning experiments

MODEL		LLAMA-7B	LLAMA-13B	LLAMA-33B
METHOD				
	OPTIMIZER			
	WARMUP RATIO			
	LR SCHEDULE			
FULL	BATCH SIZE		128	∖
	EPOCHS		3	∖
	LEARNING RATE		2E-5	∖
	WEIGHT DECAY		0.	∖
	MAX SEQ. LENGTH		2048	∖
LORA	BATCH SIZE			128
	EPOCHS			3
	LEARNING RATE	2E-4	2E-4	1E-4
	WEIGHT DECAY			0.
	MAX SEQ. LENGTH			2048
	LORA RANK		$r_q = r_v = 128$	
LORA ALPHA			256	
SIFT	BATCH SIZE			128
	EPOCHS			3
	LEARNING RATE	2E-4	9E-5	8E-5
	WEIGHT DECAY			0.
	MAX SEQ. LENGTH			2048
	SPARSITY RATE	5%	4%	3%
SIFT MODULES				W_q, W_k, W_v, W_o

B.3. Results of differernt categories in MMLU Benchmark

Figures 7, 8, and 9 serve as a supplement to Table 3, illustrating the score comparisons for various categories on MMLU benchmark under different configurations.

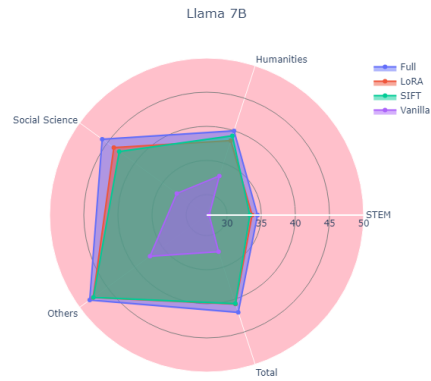


Figure 7. MMLU Evaluation results of Llama-7b fine-tuned by different methods

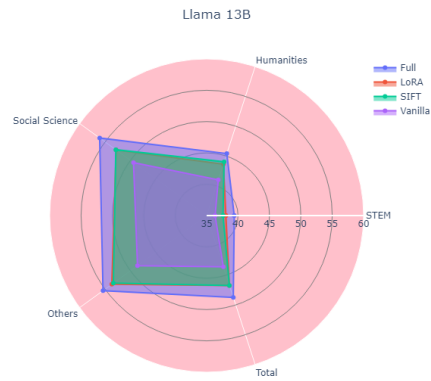


Figure 8. MMLU Evaluation results of Llama-13b fine-tuned by different methods

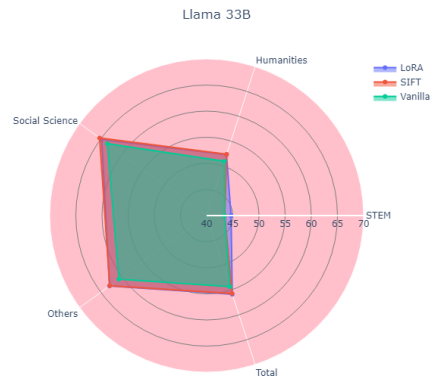


Figure 9. MMLU Evaluation results of Llama-33b fine-tuned by different methods

